Engineering the figure of merit and thermopower in single-molecule devices connected to semiconducting electrodes

D. Nozaki, H. Sevinçli, W. Li, R. Gutiérrez, and G. Cuniberti
Institute for Materials Science and Max Bergmann Center of Biomaterials, Dresden University of Technology, 01062 Dresden, Germany
(Received 19 November 2009; revised manuscript received 1 April 2010; published 3 June 2010)

We propose a possible route to achieve high thermoelectric efficiency in molecular junctions by combining a local chemical tuning of the molecular electronic states with the use of semiconducting electrodes. The former allows to control the position of the highest-occupied molecular orbital (HOMO) transmission resonance with respect to the Fermi energy while the latter fulfills a twofold purpose: the suppression of electronlike contributions to the thermopower and the cutoff of the HOMO transmission tails into the semiconductor band gap. As a result a large thermopower can be obtained. Our results strongly suggest that large figures of merit in such molecular junctions can be achieved.

DOI: 10.1103/PhysRevB.81.235406 PACS number(s): 85.80.Fi, 73.63.Rt, 81.07.Nb, 81.07.Pr

I. INTRODUCTION

Thermoelectric materials convert thermal gradients and electric fields for power conversion and for refrigeration, respectively. With the increase in energy demand, thermoelectric applications are attracting a considerable interest. Unfortunately, thermoelectrics find currently only special applications due to their limited efficiency, which is measured by a dimensionless parameter, the thermoelectric figure of merit: $ZT=S^2TG/\kappa$, which includes the Seebeck coefficient (thermopower) S, an average temperature T, the electrical conductance G, and the thermal conductance $\kappa=\kappa_{el}+\kappa_{ph}$, the latter containing both electronic κ_{el} and vibrational κ_{ph} contributions. Maximizing ZT is challenging because optimizing one physical parameter often adversely affects another.

However, as suggested in the early 1990s,[1] dimensionality reduction toward the nanoscale could provide an additional parameter to tune the electrical and thermal response of thermoelectric materials. This has triggered an active research on new nanoscaled thermoelectric materials.[2–13] An alternative to inorganic-based materials could be to exploit molecules, which have been already extensively investigated in the context of charge transport and molecular electronic applications in the past two decades.[14] Indeed, the Seebeck coefficient of different single molecules[15] as well as the thermal conductance of self-assembled monolayers[16] have been meanwhile experimentally investigated. Theoretically, only few studies on the thermoelectric properties in few level systems (molecules, small quantum dots) have been presented to date.[17–27] Concerning this "organic route," two aspects should be taken into account. First, as proposed by Mahan and Sofo,[28] the presence of a sharp resonance near the Fermi level E_F can considerably increase the thermopower since the latter depends on the derivative of the conductance near E_F. One key advantage of using molecules as potential thermoelectrics is the capability to tune their chemical and hence also their electrical and thermal properties in a *very controlled* way. The second aspect is more generic: by using *metallic* electrodes to contact a molecule, there are holelike and electronlike contributions to S arising from tunneling through the highest-occupied molecular orbital (HOMO) and lowest-unoccupied molecular orbital (LUMO) states, respectively. Both contributions appear with different signs in S and thus partially cancel each other. Is it possible to filter out electronlike (or holelike) contributions?

In this study, we propose a combination of chemical tuning of the molecular electronic structure with the use of *semiconducting* electrodes to improve the thermoelectric efficiency of molecular junctions. Such electrodes provide a way to lift the compensation of holelike and electronlike contributions to the thermopower. Specifically, if the LUMO resonance lies within the semiconductor band gap, no states are available for the "electronic" channel, which is then blocked and the thermopower will be mainly determined by the HOMO (hole) channel. In this sense, the band gap in the electrodes's electronic structure acts as a filter blocking specific contributions to the thermopower from the molecular orbitals. This together with the inclusion of donor groups in a π-conjugated molecule (chemical tuning) can lead to a dramatic increase in the thermopower of the junction by generating sharp resonances close to the Fermi level. Additionally, the presence of a band edge can further increase the log derivative of the transmission function and hence also the thermopower compared with the case of metallic electrodes.

We illustrate these ideas by using a minimal model Hamiltonian as well as a first-principles-based approach to the electronic structure and the transport properties of the molecular junctions. A typical electrode-molecule setup used in our simulations is displayed in Fig. 1. In the next section we describe our theoretical methodology, and in Sec. III results for the electronic conductance as well as for the vibrational contribution to the thermal conductance of three different molecular junctions are discussed.

II. METHODS

A. Electronic transport problem

To deal with the electronic-structure problem, we use a very efficient density-functional parametrized tight-binding approach (DFTB) (Ref. 29) which can perform on the same level as full DFT-based calculations. This approach has been combined with Green's function techniques to treat charge

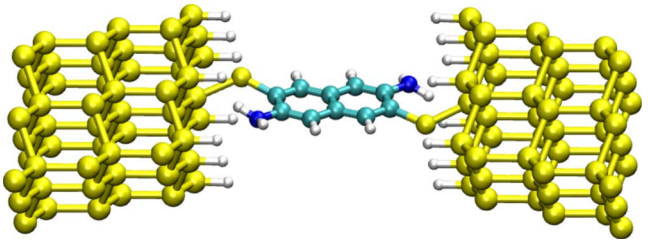

FIG. 1. (Color online) A typical molecular junction investigated in this study. Two silicon electrodes terminated at the (111) facet are bridged by a molecule. In the calculations, periodic boundary conditions in the lateral directions have been used. The electrode surface is passivated with hydrogen atoms to avoid strong structural distortions related to surface reconstruction effects.

transport in the molecular junctions of interest.[30] In a first approximation, we consider the electronic and vibrational systems to be decoupled from each other so that the electronic transport properties can be calculated within the Landauer approach, i.e., the elastic, energy-dependent transmission function $\mathcal{T}_{el}(E)$ for the molecules attached to the electrodes is evaluated and from it, the electronic component of the relevant thermoelectric coefficients at zero applied bias can be obtained. The transmission function $\mathcal{T}_{el}(E) = \mathrm{Tr}[G^r \Gamma^L G^a \Gamma^R]$ can be computed as a function of the charge injection energy E. The broadening functions $\Gamma^\alpha(\alpha = L,R)$ of the left (L) and right (R) electrodes, which encode the electrode-molecule interaction, are calculated via the self-energies $\Sigma^{r(a),\alpha}$ as $\Gamma^\alpha = i(\Sigma^{r,\alpha} - \Sigma^{a,\alpha})$. The retarded molecular Green's function (after tracing out the electrode degrees of freedom) is further given by $G^r(E)^{-1} = [(E+i0^+)I - H_m - \Sigma^{r,L} - \Sigma^{r,R}]$, I being the identity matrix, and H_m the Hamiltonian for the free molecule.

Using nonequilibrium thermodynamics, expressions for the relevant Onsager coefficients in terms of the transmission function $\mathcal{T}_{el}(E)$ can be obtained:[17,20] $L_n(T) = \int dE (E - E_F)^n [-\partial f(E,T)/\partial E] \mathcal{T}_{el}(E)$, where $f(E,T)$ is the Fermi function. The Seebeck coefficient S and the electronic part of the thermal conductance κ_{el} can then be written as

$$S(T) = (-1/eT)(L_1/L_0), \tag{1}$$

$$\kappa_{el}(T) = (2/hT)(L_2 - L_1^2/L_0). \tag{2}$$

From here, the electronic part of the figure of merit ZT_{el} is then given by $ZT_{el}^{-1} = (L_0 L_2 / L_1^2) - 1$.

B. Phonon transport problem

Concerning now the vibrational part of the thermal conductance, we follow a similar partitioning scheme to that used for the electronic problem. The system is divided into subsytems $\alpha = L$, R, or C. Using the harmonic approximation the vibrational Hamiltonian can be written as

$$H_{ph} = \sum_\alpha H_\alpha + (u^L|K^{LC}|u^C) + (u^R|K^{RC}|u^C). \tag{3}$$

Here, the first term includes $H_\alpha = 1/2(\dot{u}^\alpha|M_\alpha|\dot{u}^\alpha) + 1/2(u^\alpha|K^{\alpha\alpha}|u^\alpha)$ where $|u^\alpha)$ is the vector of coordinates whose elements u_i^α correspond to the ith degree of freedom in the α region and $(u^\alpha|$ is its transpose. Accordingly, $K_{ij}^{\alpha\beta}$ represent the coupling between mass coordinate i of subsystem α with j of subsystem β, and M_α is the diagonal matrix of corresponding atomic masses. We perform density-functional calculations using a localized orbital basis set[31] to obtain the force constants for the central region. Double-zeta-polarized basis sets are chosen for increasing the accuracy of the vibrational modes calculation. The local density approximation for the exchange-correlation functional has been used within the PW92 paramerization.[32] The atomic coordinates obtained from DFTB calculations were further optimized so that the convergence criteria for atomic forces is set to 10^{-3} eV/Å. The force constants were obtained by applying a small perturbation to each degree of freedom. For the vibrational surface Green's functions of the reservoirs, we use the approach explained in Ref. 33, which relies on the fact that the phonon surface density of states behaves linearly at low frequencies and only the phonons in this spectral range are giving the most important contribution to heat transport.

The vibrational transmission spectrum is then calculated using Green's function techniques, similar to the electronic counterpart. The retarded (advanced) Green's function of subsystem α in the absence of coupling to other subsytems is defined as $g^{r(a),\alpha}(\omega) = [(\omega \mp i0^+)^2 - D^{\alpha\alpha}]^{-1}$ with $D^{\alpha\beta} = M_\alpha^{-1/2} K^{\alpha\beta} M_\beta^{-1/2}$. When the couplings are switched on, the retarded Green's function for the central region is $G^{r,C}(\omega) = [(\omega \mp i0^+)^2 - D^{CC} - \Sigma^{r,L} - \Sigma^{r,R}]$, where $\Sigma^{r(a),\alpha} = D^{C\alpha} g^{r(a),\alpha} D^{\alpha C}$ is the retarded (advanced) self-energy due to coupling to the phonon reservoir α. The couplings give rise to broadening of vibrational modes $\Gamma_{ph}^\alpha = i(\Sigma^{r,\alpha} - \Sigma^{a,\alpha})$, and the transmission function is written as $\mathcal{T}_{ph}(\omega) = \mathrm{Tr}[G^{r,C} \Gamma_{ph}^L G^{a,C} \Gamma_{ph}^R]$. The phonon contribution to the thermal conductance at a given temperature T is then expressed as

$$\kappa_{ph}(T) = \int_0^\infty \frac{d\omega}{2\pi} \hbar\omega \frac{\partial f_B(\omega,T)}{\partial T} \mathcal{T}_{ph}(\omega). \tag{4}$$

Finally, the total figure of merit ZT can be expressed in terms of the electronic part ZT_{el} as

$$ZT = ZT_{el} \frac{\kappa_{el}}{\kappa_{el} + \kappa_{ph}} \tag{5}$$

III. RESULTS

A. A toy model

We will first illustrate our approach within a minimal model Hamiltonian in order to highlight different factors influencing the thermopower of the junction. We consider two electronic levels, which mimic the frontier orbitals of a molecule and which are coupled to semiconducting electrodes as shown in Fig. 2(a). The thermopower S and the electronic figure of merit ZT_{el} are calculated as a function of the relative position of the HOMO to the Fermi level E_F, $\Delta = E_{\mathrm{HOMO}} - E_F$, and for different coupling strengths to the

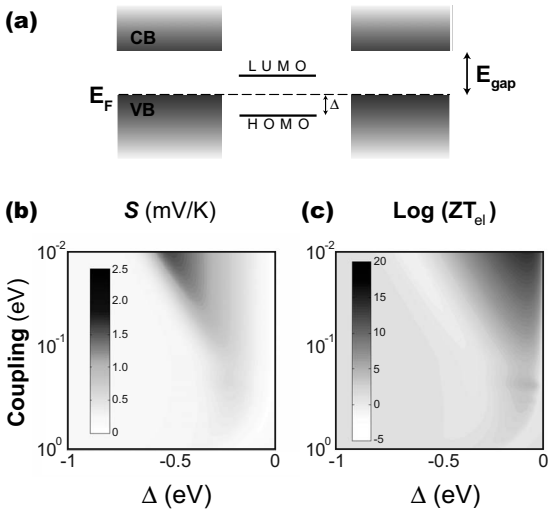

FIG. 2. Top panel: energy profile of the model semiconductor-molecule-semiconductor junction. E_{gap} is the gap between the valence and conduction bands, $\Delta = E_{\mathrm{HOMO}} - E_F$ denotes the position of the HOMO with respect to E_F. The molecular gap is chosen so as to have the LUMO level placed inside the semiconducting gap. Lower panel: (b) Seebeck coefficient S and (c) the electronic part of the thermoelectric figure of merit (ZT_{el}) as a function of Δ and the effective coupling strength to the electrodes Γ at $T=300$ K. Notice that the largest thermopower could be achieved by having a weak coupling to the electrodes (large tunnel barriers) and a molecular resonance close to the Fermi level (large derivative). Since there is no upper bound for ZT_{el}, very large values can be formally attained within these model calculations.

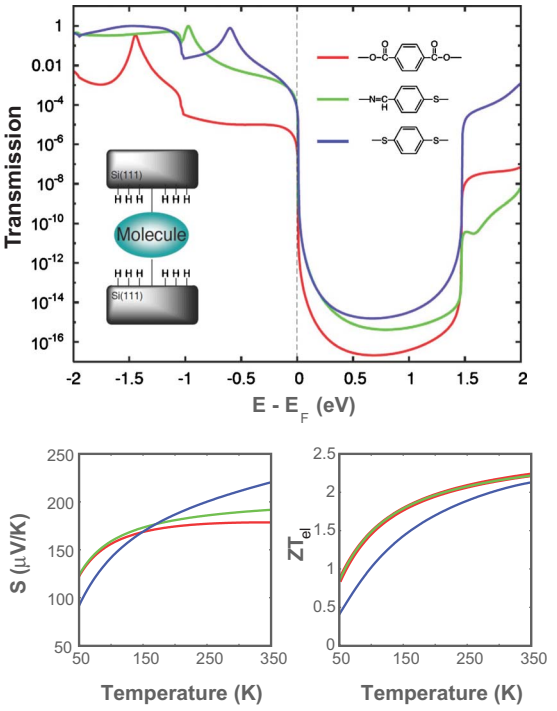

FIG. 3. (Color online) (Top panel) Zero-temperature transmission spectra of a benzene molecule sandwiched between Si electrodes via different linker groups. The position of the HOMO level is modified due to charge-transfer effects. (Bottom panel) Temperature dependence of the thermopower S (left) and corresponding figure of merit ZT_{el} (right) for the different linker groups.

electrodes. In Figs. 2(b) and 2(c), room-temperature values for S and ZT_{el} are shown. We see that it is possible to obtain S values as large as ~ 2 mV/K when the molecule-electrode coupling is ~ 10 meV, and the HOMO level is placed 0.5 eV below E_F. Even much higher values of S are possible for weaker coupling strengths. The optimum value of Δ is related to the operating temperature and it is smaller for lower temperatures.[18] Very high thermopower can be achieved with a delta-function-shaped conductance peak near to E_F for bulk systems;[28] for a model molecular system this behavior has been recently demonstrated.[18] Formally, the figure of merit has no upper bound so that arbitrarily large values can be obtained within a model approach. Though for the realistic molecular junctions we are going to consider farther below the effective electrode-molecule coupling is on average strong (~ 100 meV), the combined use of semiconducting electrodes and chemical tuning still allows for thermopower optimization.

For the sake of completeness we have also studied the thermopower in the specific case of weak coupling (Coulomb blockade) to the electrodes by using the Anderson Hamiltonian to include Coulomb interactions on the two-sites molecule. We have used nonequilibrium Green's functions to calculate the transport properties in this regime.[34] For $U \neq 0$, additional states at energies $\sim \epsilon_{\mathrm{HOMO,LUMO}} + U$ emerge; such states could be additionally tuned, thus eventually leading to a further increase in the thermopower. This however requires a separate study, see, e.g., Ref. 18.

B. Thermoelectric efficiency of single-molecule junctions

In this section we will discuss to which extent the analysis presented in the previous paragraphs can be realized in realistic molecular junctions. We have addressed two main issues: (i) the role of the linker groups in determining the relative position of the HOMO with respect to the Fermi energy and (ii) modifications of the thermopower through selective chemical doping of the molecules. The molecules are covalently attached to hydrogen-passivated Si(111) surfaces and relaxed with periodic boundary conditions parallel to the surface.[35] In each unit cell, the top/bottom silicon surfaces comprise 54 Si atoms forming three Si layers and eight hydrogen atoms covering the Si(111) surface. In order to allow for structural relaxation effects of the surface, the two outermost layers are included in the relaxation process. Figures 3 and 4 show the transmission spectra of several junctions together with the corresponding thermopower S and figures of merit ZT_{el}. In Fig. 3 the influence of different linker groups on the transmission function around the Fermi level for a benzene molecule is shown. The position of the Fermi energy in our calculations is provided by a self-consistent calculation under the constraint of global charge neutrality in the electrode-molecule system.[36]

From the figure we see that thiol linkers turn out to be the most effective linkers; they induce a high-transmission HOMO resonance around 0.5 eV below the Fermi level. Notice also the sharp suppression of the transmission tails above the conduction band edge due to the absence of spectral

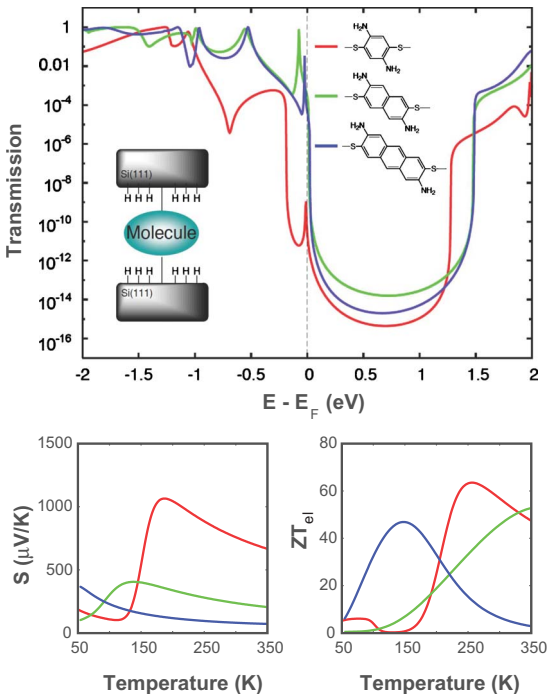

FIG. 4. (Color online) (Top panel) Zero-temperature transmission spectra of three polyacene molecules (benzene, naphtalene, and anthracene) with NH_2 side groups and attached to Si electrodes via thiol linkers. For all three molecules the HOMO level lies almost at the corresponding Fermi energy. Notice also that for the benzene molecule the HOMO state moves into the semiconductor band gap. (Bottom panel) Temperature dependence of the thermopower S (left) and figure of merit ZT_{el} (right).

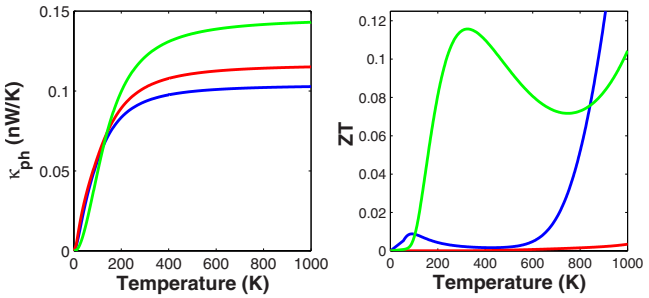

FIG. 5. (Color online) (Left panel) Vibrational thermal conductance of the three polyacene molecules (benzene, naphtalene, and anthracene) with NH_2 side groups. (Right panel) The full figure of merit ZT including the vibrational contribution of the thermal conductance.

weight in the semiconducting electrodes: this effect can additionally lead to a large derivative at the Fermi level and to a dramatic increase in S when comparing with metallic electrodes. The other linkers studied here induce larger energy shifts of the transmission resonances away from the Fermi level and thus seem to be less appropriate for the realization of an efficient thermoelectric molecular junction. The behavior of S in the lower panel of Fig. 3, which is monotonically increasing with temperature until 350 K, is related to the fact that the HOMO peaks are located away from the Fermi energy, and they are relatively broad so that higher temperatures are required for them to maximally contribute to the current. It is evident from the figure that when the peak is closer to the Fermi level (benzenedithiol) S has the highest value at room temperature. Taking the previous results into account, we have then investigated small polyacene molecules (benzene, napthtalene, and anthracene) with NH_2 functional groups added at the ortho-positions of the benzene rings, see Fig. 4. As recently shown,[22] the controlled torsional motion of side groups can help to tune the thermopower of a molecular junction; this would require however very specific mechanical manipulations at the single-molecule level. In the present study we demonstrate a different alternative route to potentially achieve high thermoelectric efficiency via pure chemical tuning of transmission resonances in combination with nonmetallic electrodes.

As it comes out from the analysis of our results, the side groups act as a chemical gate which shifts the transmission spectrum toward the Fermi level. As a result, for the three polyacene species studied the HOMO levels are essentially lying at or slightly below E_F. Moreover, due to a low spectral weight onto the linker region, the coupling of these levels to the electrodes is rather weak, leading to a narrowing of the transmission resonances closest of the frontier orbitals. Notice that in contrast to naphtalene and anthracene dithiol, the HOMO resonance of the benzene dithiol molecule has a very low transmission; this is related to the fact that the energy shift induced by the side groups moves this level into the semiconducting band gap, where no spectral support exist in the electrodes. Taking into account the narrowness of the HOMO levels together with their energetic position, we may expect a dramatic increase in the thermopower when comparing with the junctions studied e.g., in Fig. 3; this is the case as shown in the lower panel of Fig. 4, where maximum S values ranging from 400–1000 μV/K could be achieved. Also very large electronic figures of merit ZT_{el} of up to 60 at about 270 K might be ideally reached. The fact that the maximum values of S and ZT_{el} do not necessarily lie at the same temperature demonstrates that the optimization of the thermopower alone is not enough to achieve optimal figures of merit. The temperature dependence of the thermopower is more complex when the peaks are sharper (see lower panel of Fig. 4). In the case of benzene, the HOMO peak lies inside the band gap; therefore it is pinned to the Fermi level and gives rise to a sharp resonance but with a very low transmission value. The peak position makes low temperature ($T<50$ K) S values larger but at higher temperatures ($T>150$ K) S starts including contributions from lower-lying molecular levels as well. For anthracene, the HOMO peak is very close to the Fermi level and this is the reason why S (and ZT_{el}) has higher values at low temperatures. On the other hand, the HOMO peak of naphtalene is located around −0.1 eV which shifts the peak of S to higher temperatures in comparison with benzene or anthracene. Also, the transmission probability rises up to almost 1 so it is possible to use the full conducting capacity of the HOMO level.

The situation changes however upon inclusion of the vibrational contributions, see Fig. 5. First, the values of ZT are considerably reduced due to the relatively good vibrational thermal conductance. Second, it turns out now that the naphtalene junction displays the most optimal figure of merit

around room temperature while ZT is strongly reduced for the two other junctions. This is in contrast to the behavior of the electronic ZT_{el} where the benzene junction showed similar high values as naphtalene around $T=300$ K, see also Fig. 4. The reason for this different behavior can be understood as follows: the low-transmissive resonance displayed by the benzene junction almost on top of the Fermi level can give rise to very high values of the thermopower S and of ZT_{el}. These coefficients, however, only quantify how efficiently the electrical current "uses" the existing temperature difference but not the amount of created current. The benzene junction lies in the class where a very low electrical current (low transmission around the Fermi level) can nevertheless yield an optimal thermopower. However, upon the inclusion of the vibrational part of the thermal conductance, the benzene junctions appear to be less efficient, since the phonon thermal conductance is considerably larger than its electronic component.

IV. CONCLUSIONS

In summary, we have shown in this study that thermopower engineering in molecular junctions could be attained by an appropriate combination of chemical gating and the use of semiconducting electrodes. The latter provide (i) a way to eliminate the LUMO channel from the thermopower, lifting the partial cancellation of holelike and electronlike contributions, and (ii) remove tail contributions from the HOMO inside the gap, thus increasing considerably the log derivative of the transmission function around the Fermi level. The phonon thermal conductance in the studied junctions is still large, so that a total figure of merit $ZT\sim 0.1$ was obtained, despite the fact that its electronic component could be very large. In this sense, further tuning of the vibrational contributions is required. Finally, we expect that our results can be scaled up to estimate the thermoelectric efficiency of self-assembled monolayers if the molecule-molecule interactions are not very strong.

ACKNOWLEDGMENTS

The authors acknowledge fruitful discussions with O. Schmidt and Th. Dienel. This work has been supported by the Volkswagen Foundation, by the European Union under Contract No. IST-021285-2, and by the Deutsche Forschungsgemeinschaft within the priority program "Nanostructured Thermoelectrics" (Grant No. SPP 1386). We further acknowledge the Center for Information Services and High Performance Computing (ZIH) at the Dresden University of Technology for computational resources.

[1] L. D. Hicks and M. S. Dresselhaus, Phys. Rev. B **47**, 12727 (1993).
[2] A. I. Boukai, Y. Bunimovich, J. Tahir-Kheli, J.-K. Yu, W. A. Goddard III, and J. R. Heath, Nature (London) **451**, 168 (2008).
[3] A. I. Hochbaum, R. Chen, R. D. Delgado, W. Liang, E. C. Garnett, M. Najarian, A. Majumdar, and P. Yang, Nature (London) **451**, 163 (2008).
[4] D. Li, Y. Wu, R. Fan, P. Yang, and A. Majumdar, Appl. Phys. Lett. **83**, 3186 (2003).
[5] J. Lee, S. Farhangfar, J. Lee, L. Cagnon, R. Scholz, U. Gösele, and K. Nielsch, Nanotechnology **19**, 365701 (2008).
[6] T. Mori, J. Appl. Phys. **97**, 093703 (2005).
[7] N. Mingo, L. Yang, D. Li, and A. Majumdar, Nano Lett. **3**, 1713 (2003).
[8] I. Savić, D. A. Stewart, and N. Mingo, Phys. Rev. B **78**, 235434 (2008).
[9] T. T. M. Vo, A. J. Williamson, V. Lordi, and G. Galli, Nano Lett. **8**, 1111 (2008).
[10] W. Kim, J. Zide, A. Gossard, D. Klenov, S. Stemmer, A. Shakouri, and A. Majumdar, Phys. Rev. Lett. **96**, 045901 (2006).
[11] H.-K. Lyeo, A. A. Khajetoorians, L. Shi, K. P. Pipe, R. J. Ram, A. Shakouri, and C. K. Shih, Science **303**, 816 (2004).
[12] H. Sevinçli and G. Cuniberti, Phys. Rev. B **81**, 113401 (2010).
[13] A. J. Minnich, M. S. Dresselhaus, Z. F. Ren, and G. Chen, Energy Environ. Sci. **2**, 466 (2009).
[14] *Introducing Molecular Electronics*, Lecture Notes in Physics, edited by G. Cuniberti, G. Fagas, and K. Richter (Springer, Berlin, 2005), Vol. 680.
[15] P. Reddy, S.-Y. Jang, R. A. Segalman, and A. Majumdar, Science **315**, 1568 (2007).
[16] Z. Wang, J. A. Carter, A. Lagutchev, Y. K. Koh, N.-H. Seong, D. G. Cahill, and D. D. Dlott, Science **317**, 787 (2007).
[17] M. Paulsson and S. Datta, Phys. Rev. B **67**, 241403(R) (2003).
[18] P. Murphy, S. Mukerjee, and J. Moore, Phys. Rev. B **78**, 161406(R) (2008).
[19] F. Pauly, J. K. Viljas, and J. C. Cuevas, Phys. Rev. B **78**, 035315 (2008).
[20] D. Segal, Phys. Rev. B **72**, 165426 (2005).
[21] G. U. Sumanasekera, B. K. Pradhan, H. E. Romero, K. W. Adu, and P. C. Eklund, Phys. Rev. Lett. **89**, 166801 (2002).
[22] C. M. Finch, V. M. García-Suárez, and C. J. Lambert, Phys. Rev. B **79**, 033405 (2009).
[23] S.-H. Ke, W. Yang, S. Curtarolo, and H. U. Baranger, Nano Lett. **9**, 1011 (2009).
[24] J. Koch, F. von Oppen, Y. Oreg, and E. Sela, Phys. Rev. B **70**, 195107 (2004).
[25] K. Esfarjani, M. Zebarjadi, and Y. Kawazoe, Phys. Rev. B **73**, 085406 (2006).
[26] K. H. Müller, J. Chem. Phys. **129**, 044708 (2008).
[27] Y.-S. Liu, Y.-R. Chen, and Y.-Ch. Chen, ACS Nano **3**, 3497 (2009).
[28] G. D. Mahan and J. O. Sofo, Proc. Natl. Acad. Sci. U.S.A. **93**, 7436 (1996).
[29] Th. Frauenheim, G. Seifert, M. Elstner, Z. Hajnal, G. Jungnickel, D. Porezag, S. Suhai, and R. Scholz, Phys. Status Solidi B **217**, 41 (2000).
[30] A. Pecchia and A. Di Carlo, Rep. Prog. Phys. **67**, 1497 (2004).
[31] J. M. Soler, E. Artacho, J. D. Gale, A. Garcia, J. Junquera, P. Ordejón, and D. Sanchez-Portal, J. Phys.: Condens. Matter **14**, 2745 (2002).

[32] J. P. Perdew and J. Wang, Phys. Rev. B **46**, 12947 (1992).
[33] N. Mingo, Phys. Rev. B **74**, 125402 (2006).
[34] B. Song, D. A. Ryndyk, and G. Cuniberti, Phys. Rev. B **76**, 045408 (2007).
[35] D. Nozaki and G. Cuniberti, Nano Res. **2**, 648 (2009).
[36] Though doping effects are not included in our approach, a possibility to tune the position of the Fermi level and to pin it at the valence band edge could be achieved, e.g., by *p* doping. This requires, however, a more specific study (Refs. 37 and 38).
[37] K. H. Bevan, D. Kienle, H. Guo, and S. Datta, Phys. Rev. B **78**, 035303 (2008).
[38] T. Rakshit, G.-C. Liang, A. W. Ghosh, M. C. Hersam, and S. Datta, Phys. Rev. B **72**, 125305 (2005).